Cleavage of Metal–Metal Bonds in Heteronuclear Clusters. Reactions of $Os_3(\mu_3\text{-}S)(\mu_3\text{-}\eta^2\text{-}SCH_2)(CO)_8(PMe_2Ph)$ with HCl and $P(OMe)_3$

Richard D. Adams,* Nancy M. Golembeski, and John P. Selegue

Department of Chemistry, Yale University, New Haven, Connecticut 06511

Received July 20, 1981

The reactions of the cluster $Os_3(\mu_3\text{-}S)(\mu_3\text{-}\eta^2\text{-}SCH_2)(CO)_8(PMe_2Ph)$ (I), which contains a thioformaldehyde ligand, with HCl and $P(OMe)_3$ have been investigated. The reaction of I with HCl yields an addition product $HOs_3(\mu_3\text{-}S)(\mu_3\text{-}\eta^2\text{-}SCH_2)(CO)_8(PMe_2Ph)Cl$ (II), which has been characterized by X-ray crystallographic methods: space group $P2_1/c$, at 23 °C; a = 10.423 (2) Å, b = 11.014 (5) Å, c = 22.743 (9) Å, β = 101.98 (3); V = 2554 (3) Å^3; Z = 4; ρ_{calcd} = 2.72 g/cm^3. For 2689 reflections ($F_o \geq 3.0\sigma(F_o^2)$) R_1 = 0.044 and R_2 = 0.048. The molecule contains a group of three osmium atoms but only one osmium–osmium bond. The third osmium is linked to the others by a triply bridging sulfide and triply bridging thioformaldehyde ligand. The addition of HCl to I results in cleavage of one of its osmium–osmium bonds. The reaction of I with $P(OMe)_3$ yields the new molecule $Os_3(\mu_3\text{-}S)(\mu_3\text{-}\eta^2\text{-}SCH_2)(CO)_7(PMe_2Ph)[P(OMe)_3]$ (III). III was also analyzed by an X-ray crystallographic analysis: space group $P\bar{1}$, at 23 °C; a = 10.694 (2) Å, b = 11.630 (3) Å, c = 12.675 (2) Å, α = 111.16 (2)°, β = 99.63 (2)°, γ = 92.36 (2)°; V = 1441 (1) Å^3; Z = 2; ρ_{calcd} = 2.55 g/cm^3. For 4083 reflections ($F_o \geq 3.0\sigma(F_o^2)$) R_1 = 0.035 and R_2 = 0.038. III is formed from I by the substitution of one of the carbonyl ligands on the phosphine-substituted osmium atom with the $P(OMe)_3$ ligand. Thus, as in I, III contains a cluster with two osmium–osmium bonds a triply bridging sulfide ligand and a triply bridging thioformaldehyde ligand. The nature of the formations of II and III is compared in terms of probable mechanisms.

Introduction

In all examples of homogeneous catalysis involving transition-metal agents, at some point a metal complex is called upon to activate either a selected reagent, a target substrate, or both. Nucleophilic and oxidative additions[1,2] and electron-transfer[3] processes which are the principal activation steps have been well studied for mononuclear transition complexes.

Attention has recently been focused on transitional metal cluster compounds as a possible new source of homogeneous catalytic agents.[4] Once again, it can be expected that oxidative and nucleophilic additions and electron-transfer processes will play important roles in reagent and substrate activations. However, a feature that makes polynuclear metal complexes unique and chemically quite different from mononuclear ones is the existence of metal–metal bonds. Frequently, the metal–metal bonds are the weakest chemical bonds in the molecule, and as a result the basic activation processes may be altered by reaction with them. One obvious way this can happen is by cleavage of the metal–metal bond, and already much attention has been focused on nucleophilic, oxidative, and reductive cleavage of metal–metal bonds in polynuclear metal complexes.[2,5–8] Of course, if all the metal–metal bonds in the cluster are cleaved, the true catalytic agents may be only the mononuclear fragments. However, heteronuclear cluster compounds which contain a group of transition-metal atoms plus some bridging, supportive main-group element, where the bonds between the main-group element and the transition-metal atoms are stronger than the metal–metal bonds, may provide a means for circumventing cluster degradation and might even permit one to take advantage of the metal–metal bond cleavage processes in the activation of certain small molecules.[9,10]

At present, we are investigating the reactivity of such heteronuclear clusters with a variety of small molecules.[10] In this report we describe the nature of reactions of the cluster $Os_3(\mu_3\text{-}S)(\mu_3\text{-}\eta^2\text{-}SCH_2)(CO)_8(PMe_2Ph)$ (I) with HCl and $P(OMe)_3$. A preliminary report on some of this work has been published previously.[11]

Experimental Section

General Data. The compounds reported in this study showed no significant sensitivity to air. However, as a matter of routine all reactions were performed under an atmosphere of prepurified nitrogen. Hexane solvent was distilled from a sodium–benzophenone solution. $Os_3(\mu_3\text{-}S)(\mu_3\text{-}\eta^2\text{-}SCH_2)(CO)_8(PMe_2Ph)$ was prepared as previously reported.[12] All other reagents were used as purchased.

Melting points were determined by using a Thomas-Hoover apparatus and are uncorrected. Infrared spectra were recorded on a Perkin-Elmer 237B spectrophotometer and were calibrated with polystyrene. Fourier transform ^1H NMR spectra were obtained at 270 MHz on a Bruker HX270 spectrometer.

Preparation of $HOs_3(\mu_3\text{-}S)(\mu_3\text{-}\eta^2\text{-}SCH_2)(CO)_8(PMe_2Ph)Cl$ (II). A 37-mg (0.0365-mmol) sample of $Os_3(\mu_3\text{-}S)(\mu_3\text{-}\eta^2\text{-}SCH_2)(CO)_8(PMe_2Ph)$ was dissolved in 15 mL of methylene chloride.

(1) Cotton, F. A., Wilkinson, G. "Advanced Inorganic Chemistry", 4th ed.; Wiley: New York, 1980.
(2) Collman, J. P.; Hegedus, L. "Principles and Applications of Organotransition Metal Chemistry"; University Science Books: Mill Valley, CA, 1980.
(3) (a) Kochi, J. K. *Acc. Chem. Res.* **1974**, *7*, 351. (b) Lappert, M. F.; Lednor, P. W. *Adv. Organomet. Chem.* **1976**, *14*, 345.
(4) (a) Muetterties, E. L. *Science (Washington, D.C)* **1977**, *196*, 839. (b) Ugo, R. *Catal. Rev.* **1975**, *11*, 225.
(5) Meyer, T. J. *Prog. Inorg. Chem.* **1975**, *19*, 1.
(6) Kramer, G.; Patterson, J.; Poë, A.; Lily, N. *Inorg. Chem.* **1980**, *19*, 1161.
(7) Poë, A.; Malik, S. K. *Inorg. Chem.* **1979**, *18*, 1241.
(8) (a) Johnson, B. F. G.; Lewis, J.; Kilty, P. A. *J. Chem. Soc. A* **1968**, 2859. (b) Candlin, J. P.; Cooper, J. *J. Organomet. Chem.* **1968**, *15*, 230.
(9) (a) Huttner, G.; Schneider, J.; Muller, H. D.; Mohr, G.; von Seyerl, J.; Wohlfart, L. *Angew. Chem. Int. Ed. Engl.* **1979**, *18*, 76. (b) Langenback, H. J.; Vahrenkamp, H. *Chem. Ber.* **1979**, *112*, 3390. (c) Langenback, H. J.; Keller, E.; Vahrenkamp, H. *Angew. Chem., Int., Ed. Engl.* **1977**, *16*, 188. (d) Dawoodi, Z.; Mays, M. J.; Raithby, P. R. *J. Chem. Soc., Chem. Commun.* **1979**, 721.
(10) Adams, R. D.; Katahira, D. A. *Organometallics* **1981**, *1*, 0000.
(11) Adams, R. D.; Golembeski, N. M.; Selegue, J. P. *J. Organomet. Chem.* **1980**, *193*, C7.
(12) Adams, R. D.; Golembeski, N. M.; Selegue, J. P. *J. Am. Chem. Soc.* **1981**, *103*, 546.

0276-7333/82/2301-0240$01.25/0 © 1982 American Chemical Society

Table I. Crystallographic Data for X-ray Diffraction Studies

	$Os_3ClS_2PO_8C_{17}H_{14}$	$Os_3S_2P_2O_{10}C_{19}H_{22}$
(A) Crystal Data		
temp (±5 °C)	23	23
space group	$P2_1/c$, No. 14	$P\bar{1}$, No. 2
a, Å	10.423 (2)	10.694 (2)
b, Å	11.014 (5)	11.630 (3)
c, Å	22.743 (9)	12.675 (2)
α, deg	90.00	111.16 (2)
β, deg	101.98 (3)	99.63 (2)
γ, deg	90.00	92.36 (2)
V (Å^3)	2554 (3)	1441 (1)
mol wt	1047.5	1107.1
Z	4	2
ρ_{calcd}, g/cm^3	2.72	2.55
(B) Measurement of Intensity Data		
radiation	Mo Kα (0.710 73 Å)	
monochromator	graphite	
detector aperture, mm		
horizontal ($A + B \tan \theta$)		
A	3.0	
B	1.0	
vertical	4.0	
cryst faces	$\bar{2}\bar{1}0$, $21\bar{2}$, $0\bar{1}2$	$10\bar{1}$, $41\bar{4}$, $0\bar{1}2$
	$01\bar{2}$, $2\bar{1}\bar{4}$, $\bar{2}14$	$01\bar{2}$, 011, $0\bar{1}\bar{1}$
crystal size, mm	0.12 × 0.17 × 0.17	0.12 × 0.12 × 0.21
crystal orientatn: direction, deg from ϕ axis	normal to $0\bar{1}2$, 22.0	b^*, 13.3
reflctns measd	$h,k,\pm l$	$h,\pm k,\pm l$
max 2θ, deg	50	52
scan type	moving crystal–stationary counter	
ω-scan width		
$(A + 0.347 \tan \theta)^0$	0.85	0.80
bkgd	one-fourth additional scan at each end of scan	
ω-scan rate (variable)		
max, deg/min	10.0	10.0
min, deg/min	1.3	1.3
no. of reflctns measd	4718	5310
data used ($F^2 \geq 3.0\sigma(F)^2$)	2689	4083
(C) Treatment of Data		
abs correction		
coeff, cm^{-1}	162	143
grid	10 × 10 × 8	10 × 10 × 8
transmission coeff		
max	0.22	0.33
min	0.09	0.04
P factor	0.02	0.01
final residuals		
R_1	0.044	0.035
R_2	0.048	0.038
esd of unit wt	2.44	3.40
largest shift/error value on final cycle	0.01	0.02
largest peaks in final doff fpiroer. e$^-$/Å^3	2.1	2.8

A solution of 12 M HCl–ethanol (1:1) was prepared, and 10 drops were added to the methylene chloride solution. The yellow solution was stirred 15 h at room temperature and became colorless. IR spectra showed the reaction to be complete, and the solution was then concentrated in vacuo to approximately 2-mL volume. A 5-mL sample of pentane was added, and when the mixture was cooled to −20 °C, a very pale yellow powder precipitated. Recrystallization of the pale yellow powder from CH_2Cl_2–octane solutions gave 20 mg of II as crystals: yield 52%; mp 151.0–151.5 °C; IR (ν CO), in methylene chloride) 2110 (m), 2095 (s), 2030 (s), 2022 (s), 1995 (m, br) cm^{-1}; ^{1}H NMR (δ, in $CDCl_3$) 7.41 (m, 5 H), 4.40 (d, 1 H), 3.98 (d, 1 H, $^2J_{H-H}$ = 11.0 Hz), 2.11 (d, 6 H, $^2H_{P-H}$ = 9.8 Hz), −15.12 (d, 1 H, $^2H_{P-H}$ = 8.55 Hz).

Preparation of $Os_3(\mu_3\text{-}S)(\mu_3\text{-}\eta^2\text{-}SCH_2)(CO)_7(PMe_2Ph)[P(OMe)_3]$ (III). A solution of I (68.0 mg, 0.067 mmol) and $P(OMe)_3$ (0.1 mL) in 50 mL of hexane was heated to reflux for 8 h. Infrared spectra indicated formation of a single product with no detectable intermediates. Chromatography on alumina (acid, 6% water) using benzene–hexane (3:7) gave a single yellow band. This was collected, reduced to a yellow oil, dissolved in a minimum of pentane, and precipitated at −78 °C. The product III was obtained as a yellow powder (19.2 mg, 26%): mp 155–156 °C; IR (ν (CO) in hexane) 2080 (s), 2045 (s), 2002 (s), 1995 (m), 1970 (mw) cm^{-1}; ^{1}H NMR (δ in $CDCl_3$) 7.54–7.38 (m, 5 H, C_6H_5), 3.72 (d, 9 H, $^3H_{PH}$ = 11.0 Hz OCH_3), 2.27 (dd, 1 H, $^2J_{HH'}$ = 11.4 Hz, J_{PH} = 11.1 Hz, SC*H*H′), 2.20 (d, 3 H, $^2H_{PH}$ = 11.0 Hz, PCH_3), 2.13 (d, 3 H, $^2H_{PH}$ = 10.6 Hz, PCH_3), 0.69 (dd, 1 H, $^2J_{HH'}$ = 11.4 Hz, $J_{H'P}$ = 4.9 Hz, SCH*H*′).

Crystallographic Analyses. Crystals of II and III suitable for diffraction measurements were obtained by slow crystallization from hexane solutions cooled to −20 °C. All crystals were mounted in thin-walled glass capillaries. Diffraction measurements were made on an Enraf-Nonius CAD-4 fully automated four-circle diffractometer using graphite-monochromatized Mo K$\bar{\alpha}$ radiation. Unit cells were determined and refined from 25 randomly selected reflections obtained by using the CAD-4 automatic search, center, index, and least-squares routines. For I the space group $P2_1/c$ was established from the systematic absences observed in the data. For II the space group $P\bar{1}$ was assumed and confirmed by the successful solution and refinement of the structure. Crystal data and data collections parameters are listed in Table I. All data processing was performed on a Digital PDP 11/45 computer using the Enraf-Nonius SDP program library (version 16). Absorption corrections of a Gaussian integration type were applied to the data

Table II. Final Fractional Atomic Coordinates, Thermal Parameters, and Their Esds for $HOs_3(\mu_3\text{-}S)(\mu_3\text{-}\eta^2\text{-}SCH_2)(CO)_8(PMe_2Ph)Cl$ (II)

atom	x	y	z	B,[a] Å²	atom	x	y	z	B,[a] Å²
Os(1)	0.39227 (7)	0.23765 (7)	0.11751 (3)		C(2)	0.337 (2)	0.109 (2)	0.0669 (7)	2.6 (3)
Os(2)	0.74224 (8)	0.07582 (7)	0.13494 (3)		C(3)	0.619 (2)	−0.031 (3)	0.0927 (8)	2.8 (4)
Os(3)	0.59225 (7)	0.39199 (7)	0.18016 (3)		C(4)	0.873 (2)	0.014 (2)	0.950 (8)	3.7 (4)
Cl	0.9159 (5)	0.2057 (5)	0.1880 (3)		C(5)	0.788 (2)	−0.041 (2)	0.2004 (9)	4.1 (5)
S(1)	0.5654 (5)	0.3312 (4)	0.0757 (2)		C(6)	0.580 (2)	0.408 (2)	0.2629 (8)	3.4 (4)
S(2)	0.5887 (5)	0.1710 (4)	0.1897 (2)		C(7)	0.776 (2)	0.433 (2)	0.1999 (9)	4.4 (5)
P	0.2260 (5)	0.3504 (5)	0.0554 (2)		C(8)	0.553 (2)	0.563 (2)	0.1629 (10)	5.0 (5)
O(1)	0.230 (1)	0.144 (1)	0.2034 (6)	4.9 (3)	C(10)	0.251 (2)	0.375 (2)	−0.0219 (9)	4.1 (5)
O(2)	0.295 (1)	0.027 (1)	0.0363 (6)	4.5 (3)	C(11)	0.196 (2)	0.502 (2)	0.0829 (8)	2.9 (4)
O(3)	0.545 (1)	−0.099 (1)	0.0658 (6)	5.0 (3)	C(12)	0.123 (2)	0.514 (2)	0.1261 (9)	4.8 (5)
O(4)	0.948 (2)	−0.023 (1)	0.0702 (7)	5.9 (4)	C(13)	0.101 (2)	0.631 (2)	0.1504 (11)	5.9 (6)
O(5)	0.806 (2)	−0.112 (1)	0.2374 (7)	6.3 (4)	C(14)	0.161 (2)	0.725 (2)	0.1298 (10)	4.9 (5)
O(6)	0.572 (1)	0.407 (1)	0.3118 (6)	4.7 (3)	C(15)	0.234 (2)	0.718 (2)	0.0895 (10)	5.1 (5)
O(7)	0.879 (2)	0.476 (2)	0.2102 (7)	7.1 (4)	C(16)	0.257 (2)	0.603 (2)	0.0645 (9)	4.6 (5)
O(8)	0.543 (2)	0.664 (2)	0.1549 (7)	6.8 (4)	C(17)	0.693 (2)	0.216 (2)	0.0684 (8)	2.9 (4)
C(1)	0.288 (2)	0.181 (2)	0.1693 (8)	3.1 (4)	C(9)	0.062 (2)	0.278 (2)	0.0427 (9)	4.5 (5)

atom	B(1,1)[b]	B(2,2)	B(3,3)	B(1,2)	B(1,3)	B(2,3)
Os(1)	2.24 (3)	2.03 (3)	2.79 (3)	0.01 (3)	0.70 (3)	0.16 (3)
Os(2)	2.68 (3)	2.56 (3)	3.63 (3)	0.49 (3)	0.96 (2)	0.11 (3)
Os(3)	2.69 (3)	2.15 (3)	3.44 (3)	−0.23 (3)	0.90 (2)	−0.29 (3)
P	3.0 (2)	2.6 (2)	3.1 (2)	0.4 (2)	0.6 (2)	0.2 (2)
S(1)	2.9 (2)	2.4 (2)	3.3 (2)	−0.3 (2)	0.9 (2)	0.1 (2)
S(2)	2.6 (2)	2.2 (2)	2.8 (2)	0.0 (2)	0.6 (2)	0.0 (2)
Cl	2.9 (2)	4.6 (3)	6.0 (3)	−0.3 (2)	0.4 (2)	−0.3 (3)

[a] Isotropic thermal parameters. [b] The form of the anisotropic thermal parameter is $\exp(-{}^1/_4[B(1,1)h^2a^{*2} + B(2,2)k^2b^{*2} + B(3,3)l^2c^{*2} + B(1,2)hka^*b^* + B(1,3)hla^*c^* + B(2,3)klb^*c^*])$.

for both structures. Neutral atom scattering factors were calculated by the standard procedures.[13a] Anomalous dispersion corrections were applied to all nonhydrogen atoms.[13b] Full-matrix least-squares refinements minimized the function $\sum_{hkl} w(|F_o| - |F_c|)^2$, where $w = 1/\sigma(F)^2$, $\sigma(F) = \sigma(F^2)/2F_o$, and $\sigma(F_o^2) = [\sigma(I_{raw})^2 + (PF_o^2)^2]^{1/2}/Lp$.

The structure of II was solved by the heavy-atom method. Hydrogen atom positions were calculated by assuming idealized geometry and staggered rotational conformations in the cases of the methyl groups. Hydrogen atom contributions were added to the structure factor calculations but their positions were not refined. Refinement converged with final values of the residuals being $R_1 = 0.044$ and $R_2 = 0.048$.

The structure of III was solved by the heavy-atom method. Hydrogen atom positions were calculated by assuming idealized geometry and by employing located positions whenever possible. The hydrogen atoms on the carbon atom of the thioformaldehyde ligand were located in a difference Fourier synthesis. Hydrogen atom contributions were added to the structure factor calculations, but their positions were not refined. Refinement converged with final values of the residuals being $R_1 = 0.035$ and $R_2 = 0.038$.

Final values of the fractional atomic coordinates, interatomic distances, and angles with errors obtained from the inverse matrix calculated on the final cycle of refinement for both structures are listed in Tables II–VII. Structure factor amplitudes are available for both structures (see supplementary material).

Results

The reaction of I with HCl yields a product which shows a resonance at δ −15.12 in its ^{1}H NMR spectrum. This can be attributed to a bridging metal hydride ligand that was apparently produced by protonation of one of the metal–metal bonds in I. Details of the molecular structure of II were established by a X-ray crystallographic analysis which revealed the presence also of a chloride ligand.

The molecular structure of II is shown in Figure 1. The molecule contains a group of three osmium atoms, but on the basis of their internuclear separations, Os(1)–Os(3) = 2.834 (1) Å, Os(1)···Os(2) = 4.005 (1) Å, and Os(2)···Os(3)

(13) "International Tables for X-ray Crystallography"; Kynoch Press: Birmingham, England, 1975; Vol. IV: (a) Table 2.2B, pp 99–101; (b) Table 2.3.1, pp 149–150.

Table III. Bond Distances (Å) with Esds for $HOs_3(\mu_3\text{-}S)(\mu_3\text{-}\eta^2\text{-}SCH_2)(CO)_8(PMe_2Ph)Cl$ (II)

Os(1)-Os(3)	2.834 (1)	S(1)-C(17)	1.872 (12)
Os(3)-S(1)	2.427 (3)	C(1)-O(1)	1.158 (14)
Os(3)-S(2)	2.445 (3)	C(2)-O(2)	1.167 (13)
Os(3)-C(6)	1.919 (13)	C(3)-O(3)	1.162 (14)
Os(3)-C(7)	1.926 (16)	C(4)-O(4)	1.130 (14)
Os(3)-C(8)	1.952 (16)	C(5)-O(5)	1.134 (15)
Os(2)-S(2)	2.457 (3)	C(6)-O(6)	1.134 (13)
Os(2)-Cl	2.423 (4)	C(7)-O(7)	1.151 (17)
Os(2)-C(17)	2.147 (12)	C(8)-O(8)	1.125 (16)
Os(2)-C(3)	1.852 (13)	P-C(9)	1.853 (15)
Os(2)-C(4)	1.911 (14)	P-C(10)	1.851 (14)
Os(2)-C(5)	1.949 (15)	P-C(11)	1.835 (12)
Os(1)-P	2.350 (3)	C(11)-C(12)	1.371 (17)
Os(1)-S(1)	2.436 (3)	C(12)-C(13)	1.441 (20)
Os(1)-S(2)	2.455 (3)	C(13)-C(14)	1.348 (20)
Os(1)-C(1)	1.864 (13)	C(14)-C(15)	1.309 (19)
Os(1)-C(2)	1.841 (12)	C(15)-C(16)	1.422 (19)
		C(11)-C(16)	1.382 (18)

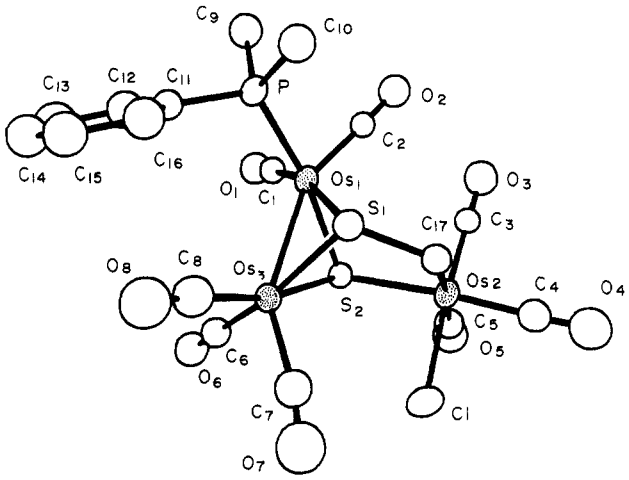

Figure 1. An ORTEP drawing of $HOs_3(\mu_3\text{-}S)(\mu_3\text{-}\eta^2\text{-}SCH_2)(CO)_8(PMe_2Ph)Cl$ (II) showing 50% electron density probability ellipsoids.

Table IV. Intramolecular Angles (Deg) with Esds for $HOs_3(\mu_3\text{-}S)(\mu_3\text{-}\eta^2\text{-}SCH_2)(CO)_8(PMe_2Ph)Cl$ (II)

Os(3)-Os(1)-S(1)	54.21 (8)	S(1)-Os(3)-C(7)	101.5 (4)
Os(3)-Os(1)-S(2)	54.49 (7)	S(1)-Os(3)-C(8)	95.4 (5)
Os(3)-Os(1)-P	111.03 (9)	S(2)-Os(3)-C(6)	89.8 (4)
Os(3)-Os(1)-C(1)	110.2 (4)	S(2)-Os(3)-C(7)	104.3 (4)
Os(3)-Os(1)-C(2)	151.6 (3)	S(2)-Os(3)-C(8)	166.7 (5)
S(1)-Os(1)-S(2)	78.74 (10)	C(6)-Os(3)-C(7)	90.9 (6)
S(1)-Os(1)-P	93.19 (12)	C(6)-Os(3)-C(8)	93.2 (6)
S(1)-Os(1)-C(1)	164.2 (4)	C(7)-Os(3)-C(8)	88.6 (6)
S(1)-Os(1)-C(2)	104.2 (3)	Os(1)-S(1)-Os(3)	71.28 (9)
S(2)-Os(1)-P	165.50 (11)	Os(1)-S(1)-C(17)	110.2 (4)
S(2)-Os(1)-C(1)	89.5 (4)	Os(3)-S(1)-C(17)	109.6 (4)
S(2)-Os(1)-C(2)	107.4 (4)	Os(1)-S(2)-Os(2)	109.24 (12)
P-Os(1)-C(1)	95.9 (4)	Os(1)-S(2)-Os(3)	70.67 (9)
P-Os(1)-C(2)	86.6 (4)	Os(2)-S(2)-Os(3)	110.90 (12)
C(1)-Os(1)-C(2)	89.4 (5)	Os(2)-C(17)-S(1)	119.7 (6)
S(2)-Os(2)-Cl	89.65 (11)	Os(1)-P-C(9)	114.2 (5)
S(2)-Os(2)-C(3)	94.6 (4)	Os(1)-P-C(10)	114.7 (5)
S(2)-Os(2)-C(4)	174.5 (4)	Os(1)-P-C(11)	115.6 (4)
S(2)-Os(2)-C(5)	88.7 (4)	C(9)-P-C(10)	102.9 (6)
S(2)-Os(2)-C(17)	88.0 (3)	C(9)-P-C(11)	103.2 (6)
Cl-Os(2)-C(3)	175.7 (4)	C(10)-P-C(11)	104.8 (6)
Cl-Os(2)-C(4)	85.0 (4)	P-C(11)-C(12)	119 (1)
Cl-Os(2)-C(5)	88.2 (4)	P-C(11)-C(16)	121 (1)
Cl-Os(2)-C(17)	88.4 (3)	C(16)-C(11)-C(12)	120 (1)
C(3)-Os(2)-C(4)	90.8 (6)	C(11)-C(12)-C(13)	121 (1)
C(3)-Os(2)-C(5)	90.8 (6)	C(12)-C(13)-C(14)	116 (1)
C(3)-Os(2)-C(17)	92.9 (5)	C(13)-C(14)-C(15)	125 (2)
C(4)-Os(2)-C(5)	92.4 (6)	C(14)-C(15)-C(16)	120 (2)
C(4)-Os(2)-C(17)	90.5 (5)	C(15)-C(16)-C(11)	118 (1)
C(5)-Os(2)-C(17)	175.2 (5)	Os(1)-C(1)-O(1)	177 (1)
Os(1)-Os(3)-S(1)	54.51 (7)	Os(1)-C(2)-O(2)	176 (1)
Os(1)-Os(3)-S(2)	54.84 (8)	Os(2)-C(3)-O(3)	178 (1)
Os(1)-Os(3)-C(6)	110.8 (4)	Os(2)-C(4)-O(4)	178 (1)
Os(1)-Os(3)-C(7)	148.2 (4)	Os(2)-C(5)-O(5)	175 (1)
Os(1)-Os(3)-C(8)	112.1 (5)	Os(3)-C(6)-O(6)	175 (1)
S(1)-Os(3)-S(2)	79.12 (10)	Os(3)-C(7)-O(7)	170 (1)
S(1)-Os(3)-C(6)	165.1 (4)	Os(3)-C(8)-O(8)	173 (2)

= 4.037 (1) Å, there is only one metal–metal bond. The group of metal atoms is held together a triply bridging sulfide ligand and a triply bridging thioformaldehyde ligand. The osmium–sulfur distances (see Table III) are similar to those found in I.[12] The sulfur atom of the thioformaldehyde ligand bridges the Os(1)–Os(3) metal–metal bond while the carbon atom is coordinated solely to Os(2). The carbon–sulfur distance, C(17)–S, at 1.872 (12) Å is very similar to that observed in I (1.869 (6) Å) and is indicative of single bond.[12] Unexpectedly, a chloride ligand was found bonded to Os(2), Os(2)–Cl = 2.423 (4) Å. The hydride ligand was not observed crystallographically but is believed to bridge the Os(1)–Os(3) bond in the cavity circumscribed by the carbonyl ligands C(1)–O(1), C(6)–O(6), and C(8)–O(8) and the phosphine ligand. I also contains eight linear terminal carbonyl ligands and a phosphine distributed in the same way as those in I. The shortest intermolecular contacts were between oxygen atoms of the carbonyl ligands and lay in the range 3.06–3.09 Å.

The reaction of I with $P(OMe)_3$ in refluxing hexane gives III as the only isolable product. Its ^1H NMR spectrum indicates the presence of a $P(OMe)_3$ ligand, but its site of coordination could not be established. This was determined, however, by the use of a X-ray crystallographic analysis.

The molecular structure of III is shown in Figure 2. Overall III is simply a trimethyl phosphite substituted derivative of I. The cluster contains three osmium atoms with two metal–metal bonds, Os(1)–Os(2) = 2.894 (1) Å, Os(1)–Os(3) = 2.837 (1) Å, Os(2)···Os(3) = 4.079 (1) Å. There is a triply bridging sulfide ligand and a triply bridging thioformaldehyde ligand. As found in I, the osmium–sulfur distances to the central osmium atom, Os(1), are significantly longer than those to external osmium atoms, Os(1)–S(1) = 2.435 (2) Å and Os(1)–S(2) = 2.448 (1) Å vs. Os(2)–S(1) = 2.393 (2) Å, Os(2)–S(2) = 2.394 (2) Å, and Os(3)–S(2) = 2.406 (2) Å. The thioformaldehyde carbon–sulfur distance, C(17)–S(1), at 1.837 (7) Å is slightly shorter than those in I and II, but this is probably not significant. The two hydrogen atoms on C(17) were located in a difference Fourier synthesis and are shown in the figure at those sites. The trimethyl phosphite ligand is coordinated to osmium Os(2), the same osmium atom which contains the dimethylphenylphosphine ligand. There are seven linear terminal carbonyl groups arranged such that Os(1) and Os(3) have three each and Os(2) has only one. The shortest intermolecular contact was between the carbonyl oxygen atoms O(2) and O(3) at 3.003 (8) Å.

Discussion

Upon reaction, I adds 1 equiv of HCl to form III in which one metal–metal bond has been cleaved. Formally, the reaction is equivalent to an oxidative addition of HCl across a metal–metal bond in I. Mechanistically, we believe the reaction occurs in a sequence of two steps: (1) a protonation of one of the metal–metal bonds in I followed by (2) a nucleophilic addition of chloride ion which induced the cleavage of the metal–metal bond. It is well-known that protonic acids will protonate metal–metal bonds in transition-metal cluster compounds, and we have observed that I will react with protonic acids containing noncoordinating counterions to give hydride-containing clusters.[15]

(14) (a) Knight, K.; Mays, M. J. *J. Chem. Soc. A* **1970**, 711. (b) Deeming, A. J.; Johnson, B. F. G.; Lewis, J. *Ibid.* **1970**, 2967. (c) Bryan, E. G.; Jackson, W. G.; Johnson, B. F. G.; Kelland, J. W.; Lewis, J.; Schorpp, K. T. *J. Organomet. Chem.* **1976**, *108*, 385.

Table V. Final Fractional Atomic Coordinates, Thermal Parameters, and Their Esds for $Os_3(\mu_3\text{-}S)(\mu_3\text{-}\eta^2\text{-}SCH_2)(CO)_7(PMe_2Ph)[P(OMe)_3]$ (III)

atom	x	y	z	B,[a] Å²	atom	x	y	z	B,[a] Å²
Os(1)	0.42952 (4)	0.13164 (4)	0.25880 (4)		C(13)	−0.1139 (12)	0.3704 (12)	0.3521 (12)	5.3 (3)
Os(2)	0.29937 (4)	0.31390 (4)	0.18958 (4)		C(14)	−0.2146 (13)	0.4056 (14)	0.2996 (13)	6.3 (4)
Os(3)	0.27106 (4)	0.15052 (4)	0.42159 (4)		C(15)	−0.1996 (15)	0.4706 (15)	0.2304 (15)	7.5 (4)
S(1)	0.4400 (3)	0.3531 (2)	0.3697 (3)		C(16)	−0.0803 (14)	0.4964 (14)	0.2066 (13)	6.3 (4)
S(2)	0.2004 (2)	0.1510 (2)	0.2313 (2)		C(17)	0.3479 (10)	0.3421 (10)	0.4764 (10)	3.2 (2)
P(1)	0.1865 (3)	0.4829 (3)	0.2356 (3)		C(18)	0.2614 (11)	0.6097 (11)	0.3698 (11)	4.4 (3)
P(2)	0.1893 (3)	0.2302 (3)	0.0034 (3)		C(19)	0.1672 (12)	0.5597 (12)	0.1330 (12)	5.0 (3)
O(1)	0.6691 (8)	0.1193 (8)	0.4190 (8)	5.2 (2)	H(12)[b]	0.0796	0.3675	0.3688	5.0
O(2)	0.5710 (10)	0.1477 (9)	0.0738 (9)	7.3 (3)	H(13)[b]	−0.1252	0.3287	0.4045	5.0
O(3)	0.3611 (8)	−0.1507 (8)	0.1458 (7)	4.8 (2)	H(14)[b]	−0.3018	0.3863	0.3066	5.0
O(4)	0.4886 (9)	0.4704 (9)	0.1316 (9)	6.7 (3)	H(15)[b]	−0.2738	0.4999	0.1940	5.0
O(5)	0.0508 (10)	0.2277 (10)	0.5482 (10)	8.4 (3)	H(16)[b]	−0.0695	0.5397	0.1537	5.0
O(6)	0.1642 (9)	−0.1263 (9)	0.3250 (9)	6.5 (2)	H(171)[b]	0.2773	0.3828	0.4648	5.0
O(7)	0.4702 (9)	0.1480 (9)	0.6185 (9)	6.4 (2)	H(172)[b]	0.4180	0.3848	0.5586	5.0
O(8)	0.2264 (8)	0.2846 (8)	−0.0870 (8)	5.3 (2)	H(181)[b]	0.3320	0.6152	0.3477	5.0
O(9)	0.0416 (7)	0.2459 (7)	−0.0281 (7)	4.7 (2)	H(182)[b]	0.2720	0.5877	0.4359	5.0
O(10)	0.2028 (8)	0.0859 (8)	−0.0534 (7)	4.9 (2)	H(183)[b]	0.2214	0.6835	0.3848	5.0
C(1)	0.5757 (9)	0.1245 (9)	0.3572 (9)	2.9 (2)	H(91)[b]	−0.0547	0.1035	−0.0449	5.0
C(2)	0.5116 (12)	0.1462 (12)	0.1419 (12)	4.9 (3)	H(92)[b]	−0.1328	0.2186	0.0099	5.0
C(3)	0.3888 (10)	−0.0435 (10)	0.1842 (10)	3.6 (2)	H(93)[b]	−0.0232	0.1895	0.0901	5.0
C(4)	0.4139 (11)	0.4097 (11)	0.1527 (11)	4.1 (3)	H(81)[b]	0.3906	0.2324	−0.0918	5.0
C(5)	0.1364 (13)	0.1986 (13)	0.5030 (12)	5.6 (3)	H(82)[b]	0.3931	0.3441	−0.1170	5.0
C(6)	0.2074 (12)	−0.0229 (12)	0.3620 (11)	4.8 (3)	H(83)[b]	0.3324	0.2160	−0.2085	5.0
C(7)	0.3902 (11)	0.1468 (11)	0.5432 (10)	3.9 (3)	H(191)[b]	0.1280	0.5042	0.0581	5.0
C(8)	0.3413 (19)	0.2668 (19)	−0.1279 (18)	10.5 (6)	H(192)[b]	0.1156	0.6273	0.1567	5.0
C(9)	−0.0519 (12)	0.1858 (12)	0.0125 (12)	5.3 (3)	H(193)[b]	0.2488	0.5949	0.1293	5.0
C(10)	0.1461 (15)	0.0146 (14)	−0.1717 (14)	7.0 (4)	H(101)[b]	0.1623	−0.0726	−0.1939	5.0
C(11)	0.0260 (10)	0.4573 (10)	0.2606 (10)	3.7 (3)	H(102)[b]	0.0542	0.0133	−0.1868	5.0
C(12)	0.0076 (12)	0.3943 (12)	0.3307 (11)	4.6 (3)	H(103)[b]	0.1780	0.0440	−0.2246	5.0

atom	B(1,1)[c]	B(2,2)	B(3,3)	B(1,2)	B1,3)	B(2,3)
Os(1)	3.02 (2)	2.37 (2)	2.64 (2)	0.43 (1)	0.45 (1)	0.85 (1)
Os(2)	2.60 (2)	2.45 (1)	2.97 (2)	0.11 (1)	0.42 (1)	1.25 (1)
Os(3)	3.99 (2)	2.72 (2)	2.97 (2)	0.25 (1)	0.92 (2)	1.24 (1)
S(1)	3.0 (1)	2.2 (1)	3.5 (1)	−0.01 (9)	0.1 (1)	0.96 (9)
S(2)	3.0 (1)	2.3 (1)	3.1 (1)	−0.07 (9)	0.43 (9)	0.96 (8)
P(1)	3.4 (1)	2.5 (1)	3.7 (1)	0.3 (1)	0.2 (1)	1.21 (9)
P(2)	3.7 (1)	3.6 (1)	3.1 (1)	0.3 (1)	0.6 (1)	1.54 (9)

[a] Isotropic thermal parameters. [b] Hydrogen atom positions were not refined. [c] The form of the anisotropic thermal parameter is $\exp(^1/_4[B(1,1)h^2a^{*2} + B(2,2)k^2b^{*2} + B(3,3)l^2c^{*2} + B(1,2)hka^*b^* + B(1,3)hla^*c^* + B(2,3)klb^*c^*])$.

Table VI. Interatomic Distances (Å) with Esds for $Os_3(\mu_3\text{-}S)(\mu_3\text{-}\eta^2\text{-}SCH_2)(CO)_7(PMe_2Ph)[P(OMe)_3]$ (III)

Os(1)-Os(2)	2.894 (1)	P(1)-C(19)	1.816 (8)
Os(1)-Os(3)	2.837 (1)	C(11)-C(12)	1.371 (9)
Os(2)···Os(3)	4.079 (1)	C(12)-C(13)	1.407 (10)
Os(1)-S(1)	2.435 (2)	C(13)-C(14)	1.328 (10)
Os(1)-S(2)	2.448 (1)	C(14)-C(15)	1.371 (12)
Os(1)-C(1)	1.855 (6)	C(15)-C(16)	1.404 (11)
Os(1)-C(2)	1.897 (9)	C(16)-C(11)	1.406 (10)
Os(1)-C(3)	1.906 (7)	P(2)-O(8)	1.590 (6)
Os(2)-S(1)	2.393 (2)	P(2)-O(9)	1.597 (5)
Os(2)-S(2)	2.394 (2)	P(2)-O(10)	1.593 (5)
Os(2)-P(1)	2.294 (2)	O(8)-C(8)	1.407 (12)
Os(2)-P(2)	2.284 (2)	O(9)-C(9)	1.460 (9)
Os(2)-C(4)	1.848 (7)	O(10)-C(10)	1.436 (10)
Os(3)-S(2)	2.406 (2)	C(1)-O(1)	1.180 (6)
Os(3)-C(5)	1.897 (9)	C(2)-O(2)	1.159 (9)
Os(3)-C(6)	1.928 (8)	C(3)-O(3)	1.167 (7)
Os(3)-C(7)	1.843 (7)	C(4)-O(4)	1.170 (8)
Os(3)-C(17)	2.160 (6)	C(5)-O(5)	1.159 (9)
S(1)-C(17)	1.837 (7)	C(6)-O(6)	1.164 (8)
P(1)-C(11)	1.828 (7)	C(7)-O(7)	1.166 (7)
P(1)-C(18)	1.828 (8)	S(1)···S(2)	3.192 (2)

An intermediate like A where the hydride ligand bridges the metal–metal bond to which the osmium atom containing the electron-rich phosphine ligand is attached seems to be very likely. The chloride ion then adds to the remaining osmium atom and yields II. As the electron pair from the chloride ion is added to the metal atom, the metal–metal bond is cleaved in order to maintain that metal atom's 18-electron configuration.

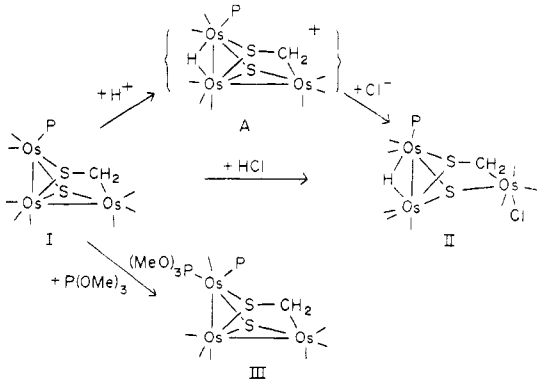

The addition of HCl to I differs significantly from the addition of HCl to the mononuclear thioformaldehyde complex $Os(\eta^2\text{-}SCH_2)(CO)_2(PPh_3)_2$.[16] In the latter reaction hydrogen is transferred to the carbon atom of the thioformaldehyde ligand and chlorine is added to the metal atom to give the methanethiolate complex $OsCl(SMe)(CO)_2(PPh_3)_2$. This reacts further with HCl to give methanethiol and $OsCl_2(CO)_2(PPh_3)_2$.

(15) Adams, R. D.; Selegue, J. P., unpublished results.

(16) Collins, T. J.; Roper, W. R. *J. Organomet. Chem.* **1978**, *159*, 73.

Table VII. Interatomic Angles (Deg) with Esds for $Os_3(\mu_3\text{-}S)(\mu_3\text{-}\eta^2\text{-}SCH_2)(CO)_7(PMe_2Ph)[P(OMe)_3]$ (III)

Os(2)-Os(1)-Os(3)	90.73 (1)	S(2)-Os(3)-C(17)	88.4 (2)
Os(2)-Os(1)-S(1)	52.49 (4)	C(5)-Os(3)-C(6)	93.0 (3)
Os(2)-Os(1)-S(2)	52.45 (4)	C(5)-Os(3)-C(7)	97.3 (3)
Os(2)-Os(1)-C(1)	139.0 (2)	C(5)-Os(3)-C(17)	90.7 (3)
Os(2)-Os(1)-C(2)	75.9 (2)	C(6)-Os(3)-C(7)	96.3 (3)
Os(2)-Os(1)-C(3)	125.0 (2)	C(6)-Os(3)-C(17)	175.6 (3)
Os(3)-Os(1)-S(1)	75.03 (4)	C(7)-Os(3)-C(17)	85.5 (3)
Os(3)-Os(1)-S(2)	53.55 (4)	Os(1)-S(1)-C(17)	97.5 (2)
Os(3)-Os(1)-C(1)	93.7 (2)	Os(2)-S(1)-C(17)	109.9 (2)
Os(3)-Os(1)-C(2)	166.6 (2)	Os(1)-S(1)-Os(2)	73.66 (5)
Os(3)-Os(1)-C(3)	93.4 (2)	Os(3)-C(17)-S(1)	107.4 (3)
S(1)-Os(1)-S(2)	81.62 (5)	Os(1)-S(2)-Os(2)	73.40 (4)
S(1)-Os(1)-C(1)	89.5 (2)	Os(1)-S(2)-Os(3)	71.52 (4)
S(1)-Os(1)-C(2)	96.6 (2)	Os(2)-S(2)-Os(3)	116.34 (6)
S(1)-Os(1)-C(3)	167.8 (2)	Os(2)-P(1)-C(18)	113.6 (2)
S(2)-Os(1)-C(1)	147.2 (2)	Os(2)-P(1)-C(19)	115.6 (3)
S(2)-Os(1)-C(2)	115.5 (2)	Os(2)-P(1)-C(11)	116.4 (2)
S(2)-Os(1)-C(3)	88.2 (2)	C(18)-P(1)-C(19)	102.2 (3)
C(1)-Os(1)-C(2)	96.8 (3)	C(18)-P(1)-C(11)	102.1 (3)
C(1)-Os(1)-C(3)	95.4 (3)	C(19)-P(1)-C(11)	105.2 (3)
C(2)-Os(1)-C(3)	94.0 (3)	P(1)-C(11)-C(12)	119.4 (5)
Os(1)-Os(2)-S(1)	53.85 (4)	P(1)-C(11)-C(16)	121.8 (6)
Os(1)-Os(2)-S(2)	54.16 (4)	C(16)-C(11)-C(12)	118.8 (7)
Os(1)-Os(2)-P(1)	148.91 (5)	C(11)-C(12)-C(13)	122.0 (7)
Os(1)-Os(2)-P(2)	111.92 (5)	C(12)-C(13)-C(14)	119.2 (8)
Os(1)-Os(2)-C(4)	109.7 (2)	C(13)-C(14)-C(15)	120.4 (9)
S(1)-Os(2)-S(2)	83.64 (5)	C(14)-C(15)-C(16)	122.2 (9)
S(1)-Os(2)-P(1)	101.42 (6)	C(15)-C(16)-C(11)	117.3 (9)
S(1)-Os(2)-P(2)	165.22 (6)	Os(2)-P(2)-O(8)	118.6 (2)
S(1)-Os(2)-C(4)	90.0 (2)	Os(2)-P(2)-O(9)	121.1 (2)
S(2)-Os(2)-P(1)	110.36 (6)	Os(2)-P(2)-O(10)	111.3 (2)
S(2)-Os(2)-P(2)	90.35 (6)	O(8)-P(2)-O(9)	92.8 (2)
S(2)-Os(2)-C(4)	163.1 (2)	O(8)-P(2)-O(10)	103.9 (3)
P(1)-Os(2)-P(2)	93.33 (6)	O(9)-P(2)-O(10)	92.0 (3)
P(1)-Os(2)-C(4)	86.2 (2)	P(2)-O(8)-C(8)	123.2 (6)
P(2)-Os(2)-C(4)	92.0 (2)	P(2)-O(9)-C(9)	119.3 (4)
Os(1)-Os(3)-S(2)	54.93 (4)	P(2)-O(10)-C(10)	121.2 (5)
Os(1)-Os(3)-C(5)	159.3 (3)	Os(1)-C(1)-O(1)	179.4 (6)
Os(1)-Os(3)-C(6)	96.3 (2)	Os(1)-C(2)-O(2)	172.9 (7)
Os(1)-Os(3)-C(7)	100.0 (2)	Os(1)-C(3)-O(3)	175.0 (6)
Os(1)-Os(3)-C(17)	79.4 (2)	Os(2)-C(4)-O(4)	178.4 (6)
S(2)-Os(3)-C(5)	107.1 (3)	Os(3)-C(5)-O(5)	177.0 (8)
S(2)-Os(3)-C(6)	88.3 (2)	Os(3)-C(6)-O(6)	174.4 (6)
S(2)-Os(3)-C(7)	154.9 (2)	Os(3)-C(7)-O(7)	176.4 (6)

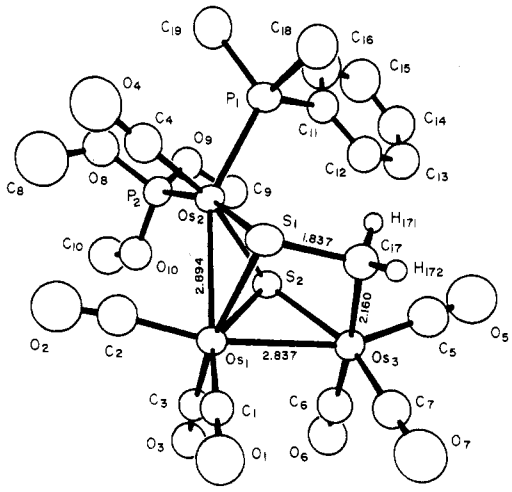

Figure 2. An ORTEP drawing of $Os(\mu_3\text{-}S)(\mu_3\text{-}\eta^2\text{-}SCH_2)(CO)_7(PMe_2Ph)[P(OMe)_3]$ (III) showing 50% electron density probability ellipsoids. Atoms H(171) and H(172) are shown with artificially reduced temperature factors.

Somewhat surprisingly the addition of trimethyl phosphite to I follows a different course. The phosphite ligand apparently attacks the cluster at the phosphine-substituted osmium atom and leads to CO substitution not metal–metal bond cleavage although the traversal of a transient intermediate with a cleaved metal–metal bond cannot be ruled out at this time.

In both cases the apparent nucleophilic additions have occurred at the external osmium atoms of the cluster. This seems to be reasonable since the internal osmium atom which is bonded to two other metal atoms would probably be more electron rich than the others and thus would be less likely to accept a nucleophile. All the factors which influence which of the external osmium atoms is actually attacked by a given nucleophile cannot be ascertained at this time, but the prior addition of a proton to one of the metal–metal bonds could be an important one in the case of the addition of HCl.

Acknowledgment. This work was supported by the National Science Foundation, Grant No. CHE-8019041, the Alfred P. Sloan Foundation through a fellowship to R.D.A. and in its initial stages[11] by the Division of Basic Energy Sciences of the U.S. Department of Energy, Contract No. ER-78-S-02-4900. NMR studies were supported by Grant No. CHE-7916210 from the National Science Foundation. We wish to thank Engelhard Industries for a loan of osmium tetraoxide.

Registry No. I, 71903-66-7; II, 75269-05-5; III, 79172-17-1.

Supplementary Material Available: Listings of structure factor amplitudes for both structures (49 pages). Ordering information is given on any current masthead.